

Tensor pomeron fit to low x DIS data

S. Glazov, Minsk, 19 Mar 2019.

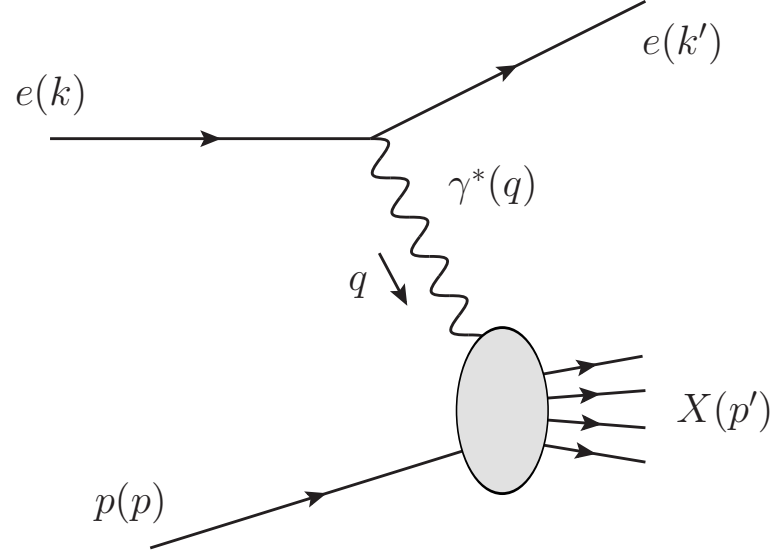
Introduction

- Low x and Q^2 data probe transition from DIS to photoproduction regime, subject to a number of phenomenological analyses.
- The data can be approximately described as a power law vs x , with power varying as a function of Q^2 . However corrections to a simple power law may lead to better fits.
- They can be also fit with a sum of two Q^2 -independent power laws, attributed to a hard and soft pomeron trajectories.
- From helicity arguments, pomeron trajectory corresponds to a symmetric rank-2 tensor exchange.
- As such, tensor pomeron model does not contain saturation. On general grounds, $\gamma^* p$ cross section does not need to obey Froissart-Martin-Lukaszuk bound since γ^* is not an asymptotic hadronic state.

arXiv:1901.08524, D. Britzger, C. Ewerz, S. Glazov, O. Nachtmann, S. Schmitt

Kinematics

Standard kinematic variables for DIS. We want to include photoproduction data, keep explicit dependence on m_p :



$$s = (p + k)^2 ,$$

$$q = k - k' ,$$

$$Q^2 = -q^2 ,$$

$$W^2 = p'^2 = (p + q)^2 ,$$

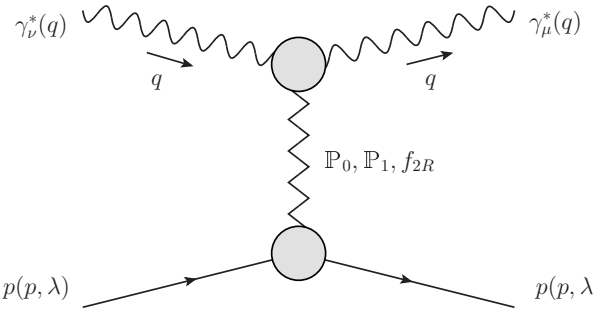
$$\nu = \frac{p \cdot q}{m_p} = \frac{W^2 + Q^2 - m_p^2}{2m_p} ,$$

$$x = \frac{Q^2}{2m_p \nu} = \frac{Q^2}{W^2 + Q^2 - m_p^2} ,$$

$$y = \frac{p \cdot q}{p \cdot k} = \frac{W^2 + Q^2 - m_p^2}{s - m_p^2} .$$

For fixed s, Q^2 , large W corresponds to large $0 \leq y \leq 1$ and small $0 \leq x \leq 1$.

Formalism



\leftarrow Forward virtual Compton scattering amplitude.

Cross sections for virtual photon scattering:

$$\sigma_T(W^2, Q^2) = \frac{2\pi m_p}{W^2 - m_p^2} e^2 W_1(\nu, Q^2), \quad (\text{recall that } F_i = \nu W_i)$$

$$\sigma_L(W^2, Q^2) = \frac{2\pi m_p}{W^2 - m_p^2} e^2 \left[W_2(\nu, Q^2) \frac{\nu^2 + Q^2}{Q^2} - W_1(\nu, Q^2) \right].$$

Structure functions using reggeon, and two tensor pomeron trajectories:

$$W_1(\nu, Q^2) = \frac{1}{2\pi m_p W^2} \sum_{j=0,1,2} 3\beta_{jpp} (W^2 \tilde{\alpha}'_j)^{\epsilon_j} \cos\left(\frac{\pi}{2} \epsilon_j\right)$$

$$\times \left[\hat{b}_j(Q^2) (4(p \cdot q)^2 + 2Q^2 m_p^2) - 2Q^2 \hat{a}_j(Q^2) (4(p \cdot q)^2 + Q^2 m_p^2) \right]$$

$$W_2(\nu, Q^2) = \frac{m_p}{2\pi W^2} \sum_{j=0,1,2} 3\beta_{jpp} (W^2 \tilde{\alpha}'_j)^{\epsilon_j} \cos\left(\frac{\pi}{2} \epsilon_j\right) 4Q^2 \hat{b}_j(Q^2).$$

Low Q^2 and low x limits

For $Q^2 = 0$, σ_L vanishes and

$$\begin{aligned}\sigma_T(W^2, 0) &= \sigma_{\gamma p}(W^2) \\ &= 4\pi\alpha_{\text{em}} \frac{W^2 - m_p^2}{W^2} \sum_{j=0,1,2} 3\beta_{jpp} (W^2 \tilde{\alpha}'_j)^{\epsilon_j} \cos\left(\frac{\pi}{2} \epsilon_j\right) \hat{b}_j(0).\end{aligned}$$

For $W^2 \gg Q^2 \gg m_p^2$,

$$\sigma_T(W^2, Q^2) \cong 4\pi\alpha_{\text{em}} 3\beta_{0pp} (W^2 \tilde{\alpha}'_0)^{\epsilon_0} \cos\left(\frac{\pi}{2} \epsilon_0\right) [\hat{b}_0(Q^2) - 2Q^2 \hat{a}_0(Q^2)],$$

$$\sigma_L(W^2, Q^2) \cong 4\pi\alpha_{\text{em}} Q^2 3\beta_{0pp} (W^2 \tilde{\alpha}'_0)^{\epsilon_0} \cos\left(\frac{\pi}{2} \epsilon_0\right) 2\hat{a}_0(Q^2),$$

and

$$\frac{\sigma_L(W^2, Q^2)}{\sigma_T(W^2, Q^2)} \cong \frac{2Q^2 \hat{a}_0(Q^2)}{\hat{b}_0(Q^2) - 2Q^2 \hat{a}_0(Q^2)}.$$

o.e. $\sigma_L(W^2, Q^2)$ determines the function $\hat{a}_0(Q^2)$ while
 $\sigma_T(W^2, Q^2) + \sigma_L(W^2, Q^2)$ determines the function $\hat{b}_0(Q^2)$

Parameterisation

	parameter	default value used	fit result
P_0	intercept		$\alpha_0(0) = 1 + \epsilon_0$ $\epsilon_0 = 0.3008^{(+73)}_{(-84)}$
	W^2 parameter	$\tilde{\alpha}'_0 = 0.25 \text{ GeV}^{-2}$	
	pp coupling parameter	$\beta_{0pp} = 1.87 \text{ GeV}^{-1}$	
P_1	intercept		$\alpha_1(0) = 1 + \epsilon_1$ $\epsilon_1 = 0.0935^{(+76)}_{(-64)}$
	W^2 parameter	$\tilde{\alpha}'_1 = 0.25 \text{ GeV}^{-2}$	
	pp coupling parameter	$\beta_{1pp} = 1.87 \text{ GeV}^{-1}$	
f_{2R}	intercept		$\alpha_2(0) = 0.485^{(+88)}_{(-90)}$
	W^2 parameter	$\tilde{\alpha}'_2 = 0.9 \text{ GeV}^{-2}$	
	pp coupling parameter	$\beta_{2pp} = 3.68 \text{ GeV}^{-1}$	

Fix W^2 and pp coupling parameters, fit intercepts. Couplings $\hat{a}_j(Q^2)$ and $\hat{b}_j(Q^2)$ are parameterized using spline functions and determined from the fit (22 parameters in total). For the f_{2R} contribution, σ_L is set to 0 ($\hat{a}_2 = 0$).

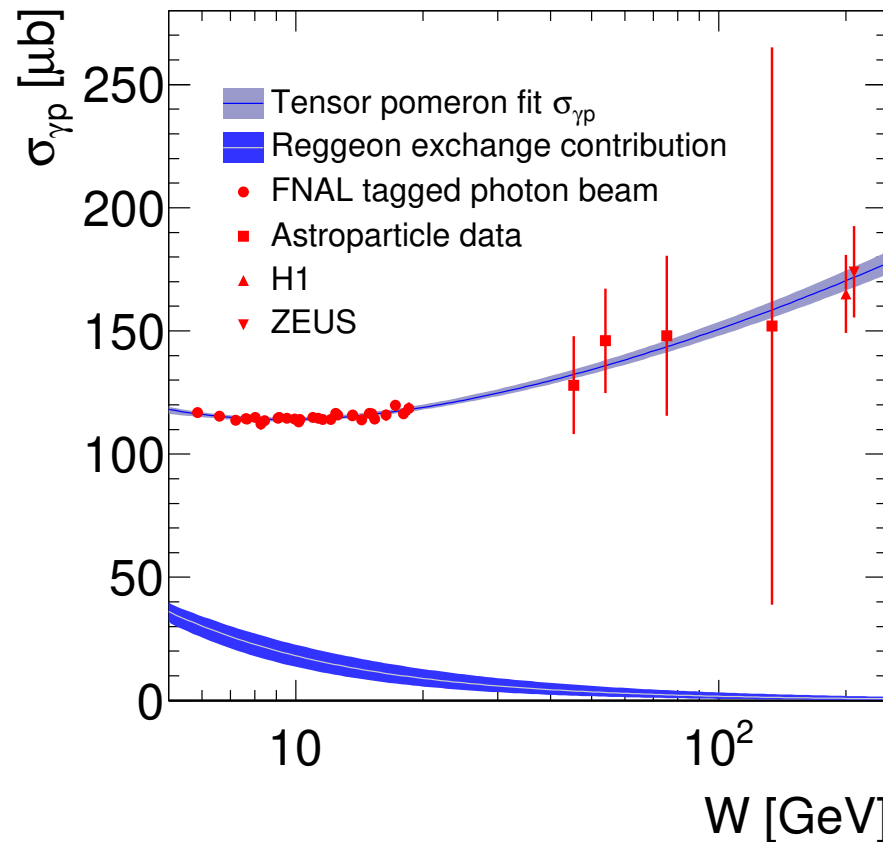
→ TensorPomeron branch in xFitter, main analysis in ALPOS

Fit to data

dataset	χ^2	number of points
DIS $\sqrt{s} = 225 \text{ GeV}$	104.98	91
DIS $\sqrt{s} = 251 \text{ GeV}$	113.12	118
DIS $\sqrt{s} = 300 \text{ GeV}$	60.38	71
DIS $\sqrt{s} = 318 \text{ GeV}$	271.82	245
HERA DIS data, all \sqrt{s}	553.77	525
H1 photoproduction	0.23	1
ZEUS photoproduction	0.03	1
cosmic ray data	0.62	4
tagged photon beam	33.29	30
all datasets	587.94	$N_{DF} = (561 - 25)$, probability 6.0%

- Fit to photoproduction and DIS data for $0 \leq Q^2 \leq 50 \text{ GeV}^2$.
- For HERA data, require $x < 0.01$, neglect valence quarks.

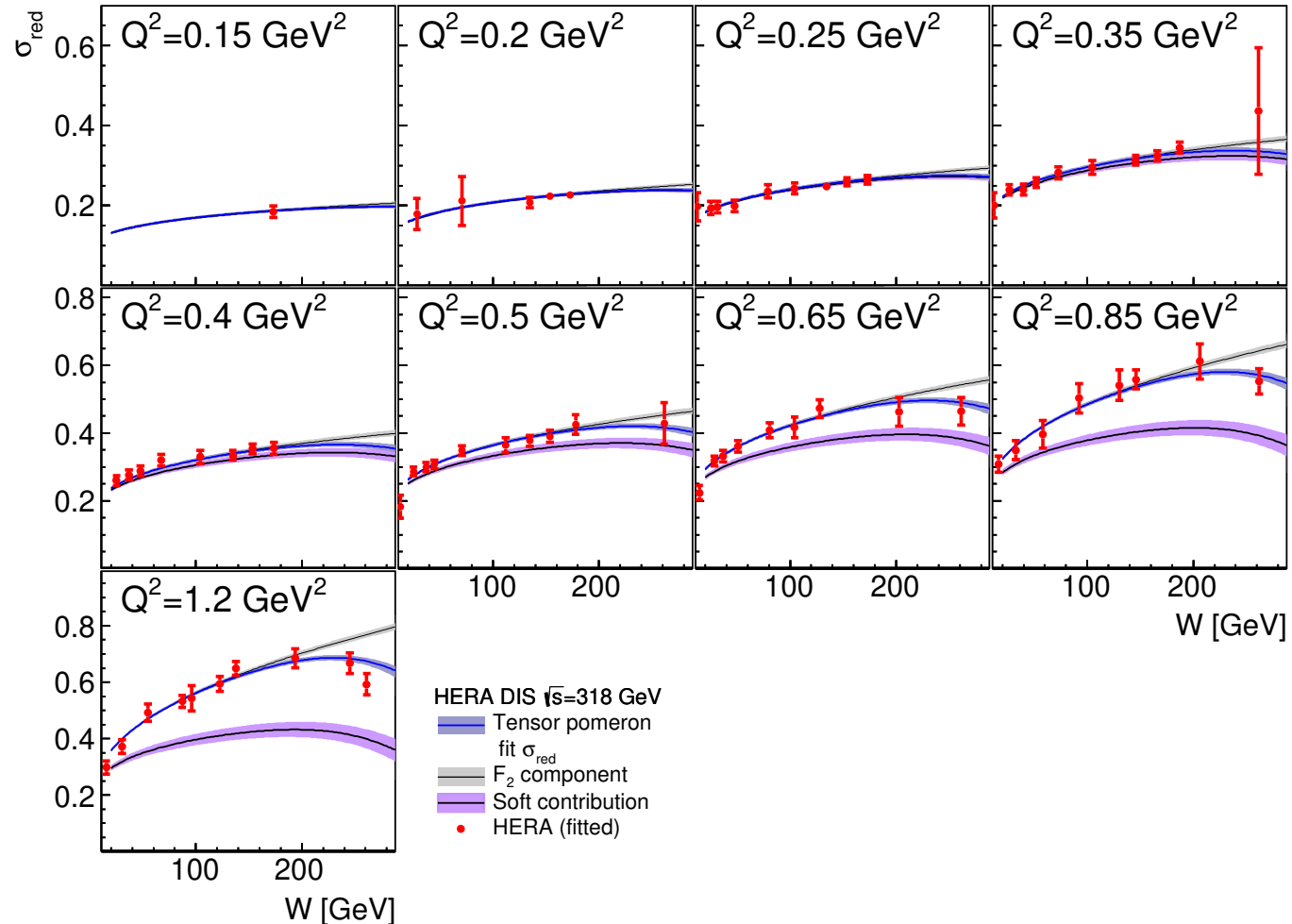
Photoproduction data



- Large W dominated by soft pomeron contribution
- Visible contribution of reggeon at low W .

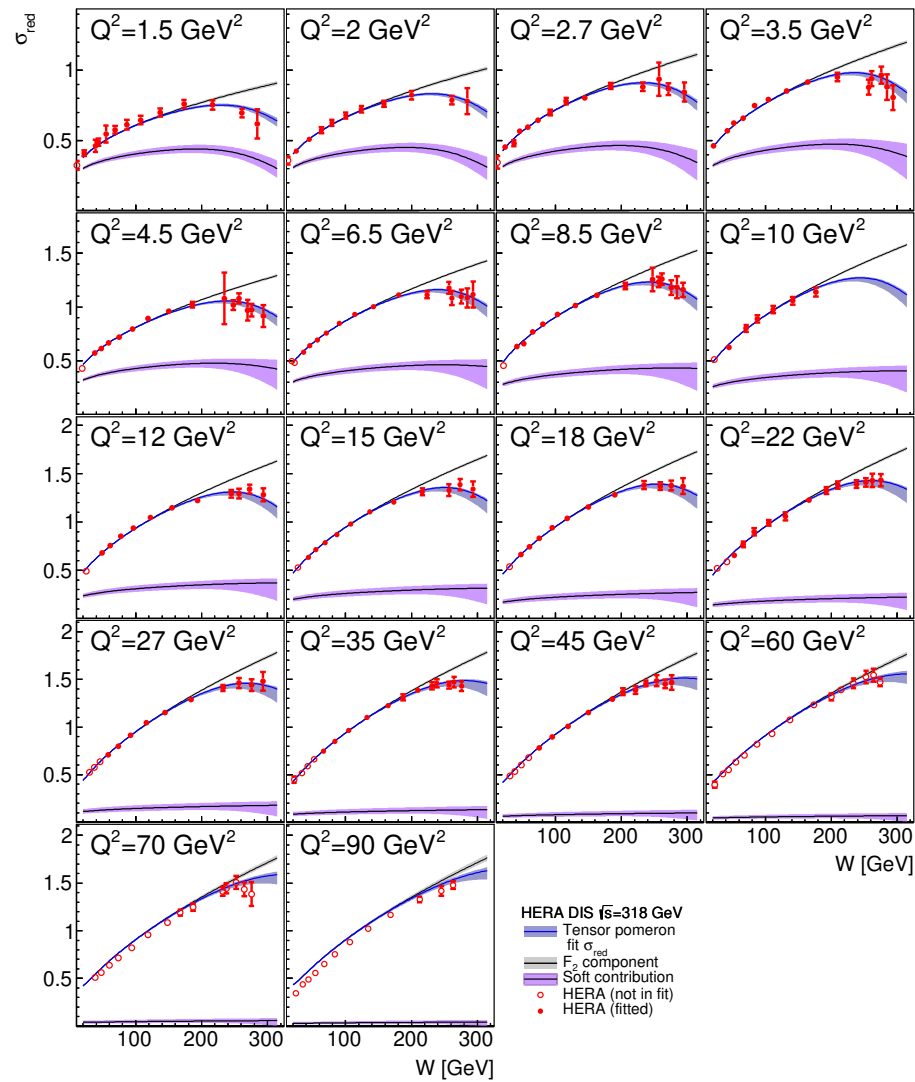
(band: here ALPOS Hesse, for xFitter Hesse or Iterate)

DIS: low Q^2



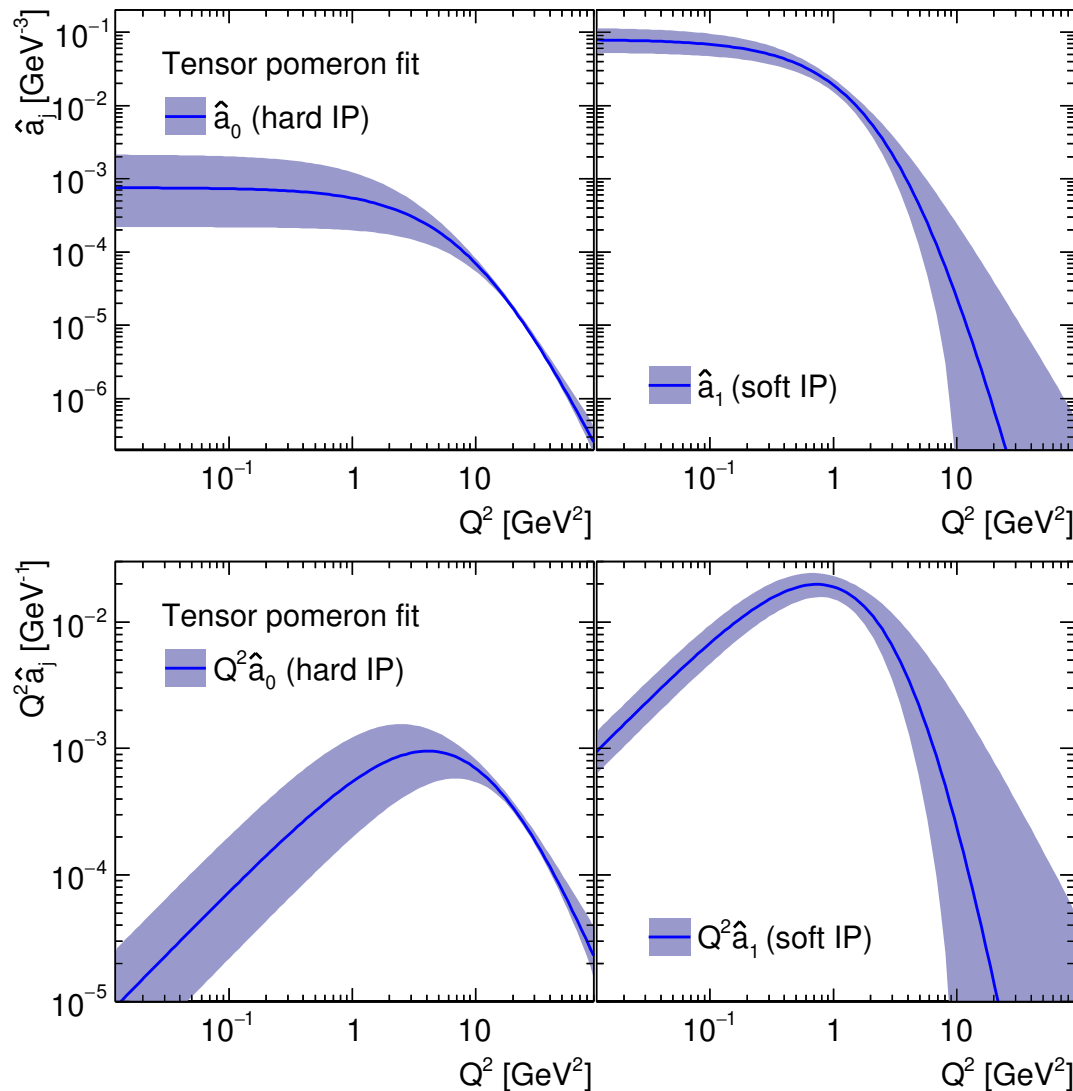
- Low Q^2 dominated by the soft pomeron component.
- Hard pomeron becomes significant from $Q^2 \geq 0.5 \text{ GeV}^2$.

DIS: high Q^2



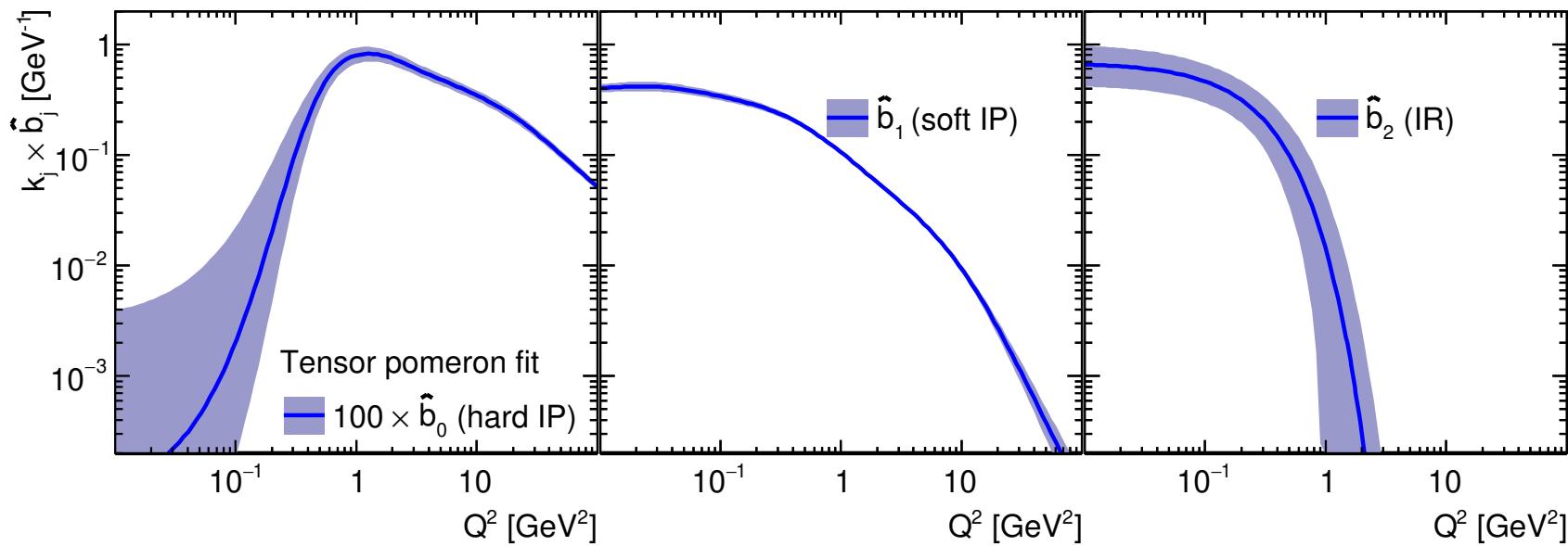
- Mix of soft and hard contributions at low Q^2 , soft contribution remains significant up to $Q^2 \sim 25 \text{ GeV}^2$
- Data are fitted up to $Q^2 = 45 \text{ GeV}^2$, low W data are removed by $x < 0.01$ cut.
- Large bend-over of the cross section at large W , due to F_L contribution.

Q^2 dependence of pomeron couplings \hat{a}_j



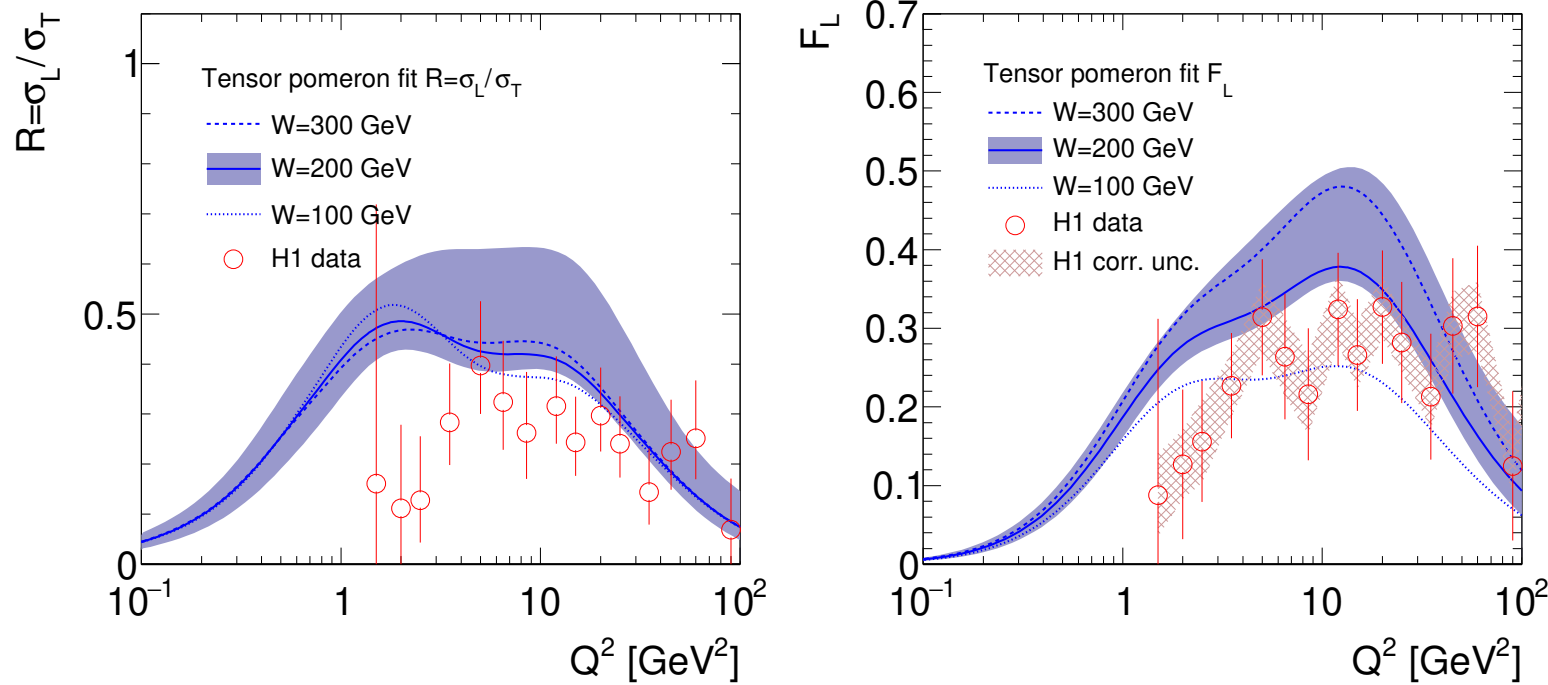
- Recall that $Q^2 \hat{a}_j$ correspond to σ_L
- Reggeon contribution is set to zero
- $\hat{a}_{0,1}$ becomes flat at low Q^2
- Soft pomeron $Q^2 \hat{a}_1$ peaks at $Q^2 \sim 1$, generating large σ_L

Q^2 dependence of pomeron couplings \hat{b}_j



- Recall that \hat{b}_j corresponds to $\sigma_T + \sigma_L$, i.e. structure function F_2 .
- Hard pomeron vanishes at $Q^2 = 0$, soft: at $Q^2 > 50 \text{ GeV}^2$ and reggeon at $Q^2 \sim 1 \text{ GeV}^2$.

Structure function F_L and ratio R



- Instead of comparing predictions to cross sections at different CME, one can compare to the measured structure function F_L or ratio $R = F_L/(F_2 - F_L)$. Note that these data are determined from the same fitted cross sections.
- For F_L , sizable dependence of predictions on W (HERA result is for $W \sim 200 \text{ GeV}^2$).
- Some tension at low Q^2 , however data uncertainties have sizable correlated component.

Summary

- Fit to DIS and photoproduction data at low x using tensor pomeron model (implemented in ALPOS and xFitter).
- Overall fit quality is good, with p -value of 6%: model without saturation can describe data up to photoproduction limit.
- Pomeron and reggeon slope parameters are consistent with other determinations.
- Driven by turn-over of the cross section at high W , fit return large value of F_L , in some tension with direct measurement.